Proceedings of the 9th U.S. National and 10th Canadian Conference on Earthquake Engineering
Compte Rendu de la 9ième Conférence Nationale Américaine et
10ième Conférence Canadienne de Génie Parasismique
July 25-29, 2010, Toronto, Ontario, Canada • Paper No 1086

REDUCED LINK SECTIONS FOR IMPROVING THE DUCTILITY OF ECCENTRICALLY BRACED FRAME LINK-TO-COLUMN CONNECTIONS

Jeffrey W. Berman[1], Taichiro Okazaki[2], and Heidrun O. Hauksdottir[3]

ABSTRACT

Previous research has shown that link-to-column connections are prone to failure at low drift levels, due to their susceptibility to fracture at the link flange to column welds. To improve the ductility of these critical details, the application of the reduced beam section concept for links in eccentrically braced frames to enhance the ductility of link-to-column connections is investigated. A design procedure for link section reduction is proposed and a finite element is developed and verified. A parametric study performed on an array of links having various cross-sections and lengths suggests that the reduced link section may substantially reduce the plastic flange strains at the link ends, which can improve the fracture life. The reduction in plastic flange strains is found to be significant for all links, with larger reductions for intermediate and flexural links. Further, the detrimental kinking deformation of the flanges, caused by the large rotation demands in shear links, is moved away from the column face when reduced sections were used. While the analysis results show promise, experimental verification is recommended before the proposed design procedure can be implemented in practice.

Introduction

Eccentrically braced frames (EBFs) combine the high elastic stiffness of concentrically braced frames (CBFs) and the high ductility and stable energy dissipation capacity of moment resisting frames (MRFs). The design rules in the AISC Seismic Provisions for Structural Steel Buildings (AISC 2005a), referred to as *The Provisions* herein, intend to achieve ductile behavior of EBFs by concentrating inelastic deformation in the links while the adjacent framing remains essentially elastic. The concentrated inelastic deformation causes significant strain demands in the link flanges at the ends of the links. Therefore, for EBF configurations where the link is connected to a column at one end, premature failure of the link-to-column connection is a major concern. Both the D and V-braced frames have links that are connected directly to the columns. Such EBF configurations are appealing for architects as they provide multiple locations for placement of doors and hallways. However, the absence of prequalified details makes link-to-column connections difficult and costly to implement.

[1]Assistant Professor, Dept. of Civil and Environmental Engineering, University of Washington, Seattle, WA 98195-2700. E-mail: jwberman@u.washington.edu
[2]Researcher, Hyogo Earthquake Engineering Research Center (E-Defense), Miki, Hyogo, Japan. Email: tokazaki@bosai.go.jp
[3]Engineer, EFLA Engineers and Consulting Co., Reykjavik, Iceland.

Recent research performed by Okazaki et al. (2006) demonstrated that several different post-Northridge moment resisting connection details that performed well in beam-to-column connections may not provide adequate ductility when used as link-to-column connections. The connections tested by Okazaki et al. included a detail following the pre-Northridge practice but implementing modifications in the welding procedure, free flange connections (Choi et al. 2003), and connections that achieve complete joint penetration groove welds without using weld-access holes, but did not include reduced beam section (RBS) connections. These test results and associated finite element analysis studies (Okazaki 2004) suggest that EBF link-to-column connections are very susceptible to fracture at the link flange to column groove welds.

A reduced link section (RLS) near the link end, similar to the RBS beam-to-column connection, may be applied to move the location of severe stresses and plastic strains away from the link end and the critical flange-to-column welds. The AISC Prequalified Connections for Special and Intermediate Steel Moment Resisting Frames for Seismic Applications (AISC 2005b), referred to as *Prequalified Connections* herein, prescribes geometric limits for RBS beam-to-column connections in terms of the parameters *a*, *b* and *c* shown in Fig. 1; however, these limits may need modification for application in RLSs due to the high moment gradient. This paper first describes a proposed design methodology for RLSs; then a parametric study, based on cyclic loading analyses of representative links, is used to investigate the impact of the geometry parameters, *a*, *b* and *c* shown in Fig. 1, on the critical flange strains. Finally, conclusions and recommendations for further research are given.

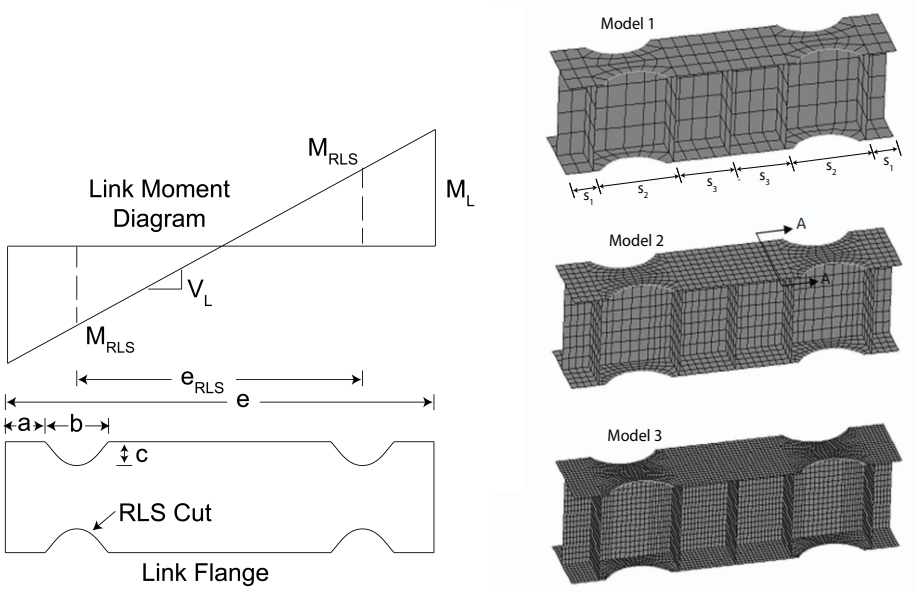

Figure 1. Link moment diagram, reduced link geometry, stiffener layout and mesh refinements.

Reduced Link Sections

The RBS is designed to limit the moment at the column face to less than or equal to the plastic moment of the beam, M_p. Dimensions *a*, *b*, and *c* in Fig. 1 are constrained by *Prequalified Connections* to be within the limits: $0.5b_{bf} \le a \le 0.75b_{bf}$, $0.65d \le b \le 0.85d$, $0.1b_{bf} \le c \le 0.25b_{bf}$, where b_{bf} is the beam flange width, and *d* is the beam depth. These limits are based on the RBS cuts used in reported test specimens, and attempt to strike a balance between constructability,

RBS effectiveness in reducing demands at the column face and control of stress concentrations in the RBS region itself. This concept may be applied to links in EBFs by using the link moment diagram and dimensions in Fig. 1. It is acknowledged that the end moments may not equalize in shear links with one end connected to a column and the other end connected to a beam-brace joint (Kasai and Popov 1986). However, this paper neglects the effect of unequal end moments for simplicity.

The authors suggest sizing the RLS to satisfy two conditions. First, the link end moment should be limited to some portion of the unreduced plastic moment capacity, M_p:

$$M_L \le \xi M_p \tag{1}$$

where ξ is the desired ratio of M_L to M_p. Second, the yielding behavior of the link should not be altered by the introduction of the RLS. The yielding behavior of EBF links is governed by the normalized link length, ρ, defined as:

$$\rho = \frac{e}{M_p / V_p} \tag{2}$$

where links with $\rho \le 1.6$ are shear links that yield primarily in shear and should be able to develop a plastic rotation as large as 0.08 rads, links with $\rho \ge 2.6$ are flexural links that yield primarily in flexure and may develop a plastic rotation of 0.02 rads, and links with $1.6 \le \rho \le 2.6$ are intermediate links that yield in a combination of shear and flexure and whose plastic rotation capacity is interpolated from the above limits. For the design of RLSs, a second normalized link length, ρ_{RLS}, is defined as:

$$\rho_{RLS} = \frac{e_{RLS}}{M_{RLS} / V_p} \tag{3}$$

where e_{RLS} is the center-to-center distance between RLSs as shown in Fig. 3. It is assumed that ρ_{RLS} dictates the yielding behavior of segment e_{RLS} in the same way ρ dictates yielding for an unreduced link with length e. In other words, to ensure that the RLS does not alter the yielding behavior of the link, ρ_{RLS} must be in the same link classification as ρ, or:

$$\begin{gathered} \textit{for Shear Links}: M_{RLS} \ge \frac{V_p e_{RLS}}{1.6} \qquad \textit{for Intermediate Links}: \frac{V_p e_{RLS}}{1.6} > M_{RLS} \ge \frac{V_p e_{RLS}}{2.6} \\ \textit{for Shear Links}: M_{RLS} < \frac{V_p e_{RLS}}{2.6} \end{gathered} \tag{4}$$

Considering link equilibrium, the following relationship between M_L and M_{RLS} that is valid for links of any length can be derived:

$$M_{RLS} \le \frac{\xi M_p e_{RLS}}{e} \tag{5}$$

The RLS geometry may be determined based on a reduced plastic strength, M_{RLS}, that satisfies these conditions, as:

$$Z_{RLS} = Z \frac{M_{RLS}}{M_p} \tag{6}$$

where Z_{RLS} is the plastic section modulus at the center of the RLS, and Z is the plastic section modulus of the unreduced link section. Z_{RLS} and Z are related through dimension c (see Fig. 1) as:

$$Z_{RLS} = Z - 2ct_f\left(d - t_f\right) \tag{7}$$

The length of the RLS, b, and the distance from the end of the link to the beginning of the RLS, a, determine the center-to-center distance between the RLSs, e_{RLS} (see Fig 1), and thereby dictate the limits for M_{RLS}.

Considering the difficulty in controlling $\xi = M_L/M_p$ within the short link lengths, the largest permitted $c = 0.25b_{bf}$ might be used for the majority of RLS. Then values for a and b may be selected to satisfy the remaining design objectives. Notably, for some combinations of large required reductions (small values of ξ), small ρ_{RLS}, and deep link sections, the parameters a, b, and c may not be determined within the limits defined by *Prequalified Connections*. In such cases, the limits might be relaxed while considering the following constructability and performance constraints:

- a should be large enough to provide access for the link flange groove welds and to fit erection tabs, which are bolted to the link web, between the link end and the stiffener placed at the end of the RLS (described below).
- b should be no less than the maximum of $2c$ and $0.25d$. The former ensures that no more than 180° of a circle is present in the RLS and the latter ensures a reasonably sized radius. Both of these help to prevent a notch effect in the RLS region. Note that in the development of RBS beams, no designs were tested with $b < 0.65d$.

The radius of the RLS cut is determined by b and c, based on the same equation used for RBS connections. Finally, it should be noted that for RBS beam-to-column connections, *Prequalified Connections* require the RBS to be designed such that the moment at the column face is less than or equal to M_p of the unreduced beam. Such a design approach applied in the above procedure would be equivalent to designing for $\xi = 1.0$.

Finite Element Model and Verification

To investigate how RLS sections may be employed to efficiently reduce flange strain demands at link-to-column connections, a number of finite element models were developed using the program MSC Marc Mentat 2005r3 (MSC Software 2005). All models were extrapolated from a reference model developed for a W14x82 shear link with a length of 1,219 mm (corresponding to $\rho = 1.33$). The reference model had an RLS with a = 132 mm, b = 239 mm, and c = 64 mm, which is a combination that satisfies the bounds given by Eqs. (1), (2), and (3), and which results in $\xi = 1.0$ and $\rho_{RLS} = 1.6$. *The Provisions* require link web stiffeners to be spaced no more than 316 mm apart for this link. As indicated in Fig. 1, three spacing dimensions, s_1, s_2, and s_3, must be specified for links with RLSs. The reference link used s_1 = 102 mm, s_2 = 300 mm, and s_3 = 208 mm. As allowed by *The Provisions*, only one-sided stiffeners were used.

The model employed MSC Marc's "Type 75" shell elements, which are four-noded, linear, thick shell elements with 6 degrees of freedom and four Gauss integration points over the area. The analyses incorporated nonlinear geometry and material behavior. An updated Lagrange formulation was used to incorporate the nonlinear geometric effects, and thereby, to capture any local buckling. Although no initial imperfections were introduced, the one-sided stiffeners produced enough disturbances in symmetry to trigger inelastic local buckling. The nonlinear material behavior was modeled using the kinematic hardening rule and Von Mises yield criteria,

and adopting a trilinear Cauchy stress versus logarithmic plastic strain relationship constructed by Okazaki (2004) for ASTM A992 steel. The yield stress was set at 359 MPa. No material strength degradation or fracture was modeled, and therefore, strength degradation of the models was caused solely by local buckling. Boundary conditions were imposed at the two ends of the link: all rotational degrees of freedom were restrained; at the left end, the nodes were permitted to translate only in the axial direction of the link; and at the right end, the nodes were permitted to translate only in the transverse direction parallel to the web. A cyclic displacement history was imposed on the right end of the link to follow the loading protocol specified in Appendix S of *The Provisions*.

The reduction of plastic strain at the link end was selected as the primary parameter to judge RLS effectiveness, i.e., the difference between plastic strain for similar links with and without RLSs. A convergence study demonstrated that that in terms of the percent change in plastic strain, very similar results may be obtained from three mesh refinements considered and shown in Fig. 1 (4, 8, and 16 elements across width of flange, denoted Models 1, 2, and 3 respectively). Fig. 2 shows the shows the percent change in equivalent plastic strain at Location 4 between the link models with and without RLSs. Because the effectiveness of RLSs may be discussed in a relative sense, and considering the significant computational time benefits achieved by using Model 2 rather than Model 3, it was concluded that the meshing scheme of Model 2 is adequate for the finite element model analyses described below. Additional comparisons of global response with experimental results for links and for RBS beam-to-column further demonstrated Model 2's adequacy but are not included here for brevity (Berman et al. 2010 and Hauksdottir 2008).

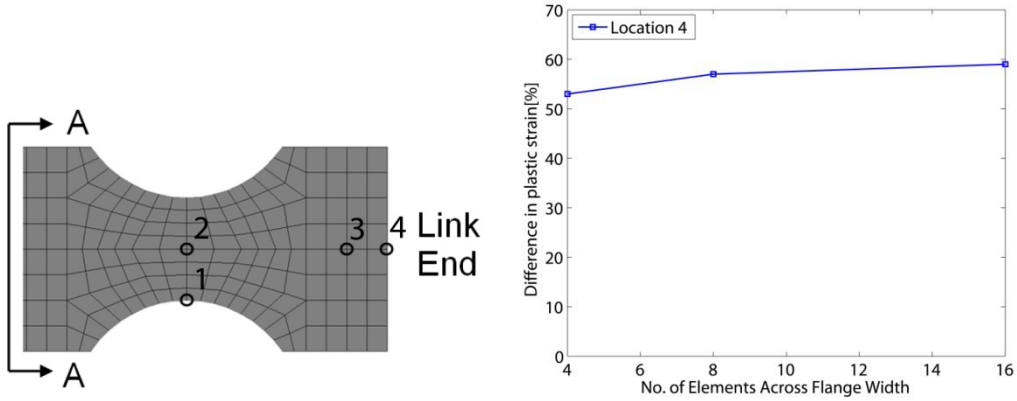

Figure 2. Convergence of percent difference in plastic strain between reduced and unreduced links at the link end vs number of elements across the link flange.

Selection of Representative Links

Table 3 presents the RLS dimensions for each link considered in the parametric study and the limiting dimensions according to the proportioning rule for RBS connections. Table 3 also shows the stiffener spacing for each link. As permitted, one-sided stiffeners were used. Dimensions s_1 and s_2 were chosen somewhat arbitrarily but such that s_2 is greater than dimension b of the RLS. Dimension s_3 was chosen to satisfy the requirements of *The Provisions*. Because flexural links do not require intermediate stiffeners between the inside edges of the RLSs, only dimensions s_1 and s_2 are listed for flexural links. For constructability and performance

considerations, the dimension a should be 102 mm (4.0 in.) or larger, the minimum value of the dimension b should be limited to the maximum of $0.25d$ or $2c$, and c should be $0.25b_f$ or smaller. However, for W12x45 shear links and W18x50 shear and intermediate links, values of a smaller than 102 mm were required to achieve the target ξ value. The proposed limits on b and c were violated in the W18x50 and W24x84 shear links designed for $\xi = 0.86$. For these two links, b was slightly smaller than $0.25d$ (the other limit $b \geq 2c$ never controlled), and c was slightly greater than $0.25b_{bf}$.

Table 1. Link properties, RLS dimensions, and stiffeners spacings for links in the parametric study.

	ξ	e (mm)	ρ_{RLS}	a (mm)	b (mm)	c (mm)	s_1 (mm)	s_2 (mm)	s_3 (mm)
				W 12x45					
AISC Min				102	200	21			
AISC Max				153	261	51			
Shear	0.86	964	1.51	95	121	51	76	159	165
$\rho = 1.3$	0.93	964	1.41	102	152	51	81	193	139
				W 12x72					
AISC Min				152	203	30			
AISC Max				229	266	76			
Shear	0.86	1261	1.51	127	178	76	102	229	203
$\rho = 1.3$	0.93	1261	1.41	152	191	76	128	263	244
Intermediate	0.86	2037	2.44	229	241	76	203	318	330
$\rho = 2.1$	0.93	2037	2.26	229	266	71	203	316	331
				W 14x82					
AISC Min				128	236	26			
AISC Max				193	309	64			
Shear	0.86	1192	1.51	102	178	64	76	239	295
$\rho = 1.3$	0.93	1192	1.41	114	216	64	76	300	234
Intermediate	0.86	1925	2.44	193	241	64	178	400	387
$\rho = 2.1$	0.93	1925	2.26	193	309	62	178	391	396
				W 18x50					
AISC Min				95	297	19			
AISC Max				143	389	48			
Shear	0.86	928	1.51	89	102	51	76	152	161
$\rho = 1.3$	0.93	928	1.41	95	114	48	76	152	161
Intermediate	0.86	1925	2.44	95	203	48	76	267	271
$\rho = 2.1$	0.93	1925	2.26	95	295	48	76	333	227
Flexural	0.86	2658	3.37	127	297	48	117	318	
$\rho = 2.9$	0.93	2658	3.12	143	389	48	127	421	
				W 18x86					
AISC Min				141	304	28			
AISC Max				212	397	71			
Shear	0.86	1265	1.51	102	191	71	76	241	212
$\rho = 1.3$	0.93	1265	1.41	114	229	71	102	269	366
Intermediate	0.86	2043	2.44	165	304	71	151	332	355
$\rho = 2.1$	0.93	2043	2.26	212	304	71	197	409	409
Flexural	0.86	2821	3.37	212	397	67	197	426	
$\rho = 2.9$	0.93	2821	3.12	212	397	60	197	426	
				W 24x84					
AISC Min				115	398	23			
AISC Max				172	520	57			
Shear	0.86	1163	1.51	102	152	64	76	203	203
$\rho = 1.3$	0.93	1163	1.41	102	165	57	76	216	195
Intermediate	0.86	1878	2.44	102	279	57	76	330	356
$\rho = 2.1$	0.93	1878	2.26	115	356	57	76	432	288
Flexural	0.86	2593	3.37	140	398	57	127	423	
$\rho = 2.9$	0.93	2593	3.12	172	470	57	152	509	

Sections W12x45, W18x50, and W24x84 present difficulties for applying the RLS proportioning rules because their webs account for a larger portion of their plastic moment capacity relative to the other sections and they have fairly short link lengths when used as shear links. To achieve a lower ξ value, the center of RLS can be moved closer to the link end by reducing a and/or b, or the plastic moment capacity of the reduced section can be reduced by increasing c. However, for sections W12x45, W18x50, and W24x84, b is constrained to be large and increasing c has limited impact on reducing the plastic moment. Flexural and intermediate links were not considered for all sections as the authors felt that some of the sections sizes with low moment of inertia values were not likely to be used as such links.

Discussion of Results

Each link in Table 1 was analyzed under the cyclic loading protocol described above. From the cyclic shear force versus plastic rotation curves for each link, a backbone curve was constructed, and the plastic rotation where the link shear force degrades to 80% of its maximum value was identified. This value, denoted the plastic rotation capacity, is plotted against the normalized link length ρ in Fig. 3a for all links considered in the parametric study. As shown, all but one link had plastic rotation capacities exceeding the maximum plastic rotation allowed by *The Provisions*. The single exception was a W18x50 link with an intermediate length (ρ = 2.1). This link exhibited severe flange and web local buckling in the RLS region, likely owing to the long RLS length (b = 295 mm = 0.65d) and correspondingly long stiffener spacing (s_2 = 333 mm = 0.73d). Therefore, flange buckling may be a concern for RLS-links, and should be controlled through a limiting value for b. Interestingly, the W12x72 intermediate and flexural links, which violated the width-thickness ratio limit for link flanges in intermediate and flexural links, did not exhibit particularly poor behavior.

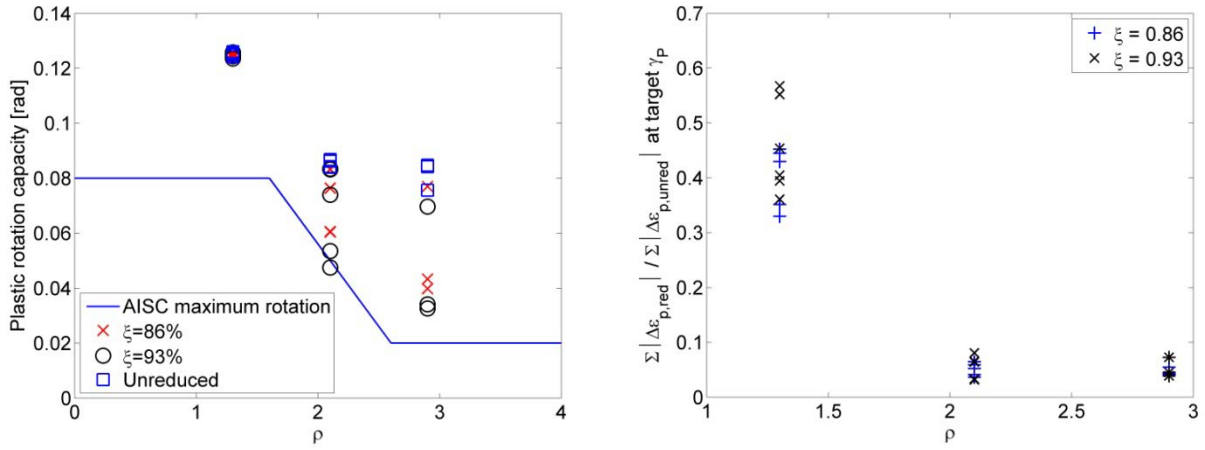

(a) (b)

Figure 3. (a) Plastic rotation vs. normalized link length for links in the parametric study. (b) Ratio of cumulative plastic strain at Point 4 in links having RLSs to that of the undreduced links vs. normalized link length.

While all links achieved their target plastic rotations, the rotation capacity is reduced for most intermediate and flexural links when RLSs are employed. The rotation capacity of shear links as limited by local buckling in the models is not significantly impacted by the presence of the RLS. There are three important points to consider when interpreting these results: (i) since

fracture was not modeled, it is likely that the plastic rotation capacity is overestimated, particularly for unreduced links that are subjected to large strain demands in the flanges at the link ends, (ii) other than the single exception, all intermediate and flexural links with RLSs were still able to reach the target rotation, and (iii) the drastic reduction in plastic strain at the link ends, shown below, indicates that the RLS is effective in mitigating fracture of intermediate and flexural links. Although not explored in this study, placement of stiffeners on both sides of the web, at the boundaries of the RLS, may improve flange, web, and lateral torsional stability of flexural and intermediate links.

Table 2 lists the longitudinal plastic strain sampled at a plastic rotation of 0.08 rad. for shear links, 0.05 rad. for intermediate links, and 0.02 rad. for flexural links, and at Locations 2 and 4 as indicated in Fig. 2. The values are listed for the two RLS-links (ξ = 0.86 and 0.93) and corresponding undreduced links. The results indicate that the RLS may reduce the flange strain for a wide variety of links. The RLS produced excellent results for intermediate and flexural links: by using either ξ = 0.86 and 0.93, the RLS practically precluded yielding at the link ends, and moved the region of plastic hinging into the RLS. The RLS is less effective for shear links but still significantly reduced the flange strains by 50-75%, with ξ = 0.86 leading to slightly larger reductions than ξ = 0.93.

Table 2. Strains at critical locations at the target plastic rotation levels for reduced and unreduced links in the parametric study.

	Location 2		Location 4		
Section	ξ = 0.86	ξ = 0.93	ξ = 0.86	ξ = 0.93	Unreduced
Shear Links at γ_p = 0.08					
W12x45	0.0247	0.0308	0.0148	0.0139	0.0278
W12x72	0.0313	0.0180	0.0084	0.0134	0.0308
W14x82	0.0454	0.0397	0.0093	0.0094	0.0371
W18x50	0.0682	0.0486	0.0206	0.0210	0.0401
W18x86	0.0477	0.0376	0.0128	0.0142	0.0369
W24x84	0.0829	0.0595	0.0188	0.0203	0.0463
Intermediate Links at γ_p = 0.05					
W12x72	0.0682	0.0555	0.0025	0.0032	0.0882
W14x82	0.1048	0.0992	0.0038	0.0040	0.1102
W18x50	0.1062	0.0826	0.0064	0.0022	0.1162
W18x86	0.1017	0.1047	0.0022	0.0019	0.1133
W24x84	0.1014	0.0840	0.0055	0.0051	0.1298
Flexural Links at γ_p = 0.02					
W18x50	0.0491	0.0450	0.0009	0.0008	0.0491
W18x86	0.0586	0.0515	0.0016	0.0024	0.0429
W24x84	0.0436	0.0439	0.0011	0.0010	0.0587

Fig. 3b shows the ratio of cumulative plastic strain at Location 4 for RLS-links to that of the unreduced links, versus the normalized link length. The data is grouped by ξ value. As shown, the ξ value has little impact on the reduction of flange strains for intermediate and flexural links; however, for shear links there is a clear dependence on ξ. Based on these results and the fact that RBS beams in SMRFs are designed for ξ = 1.0, relaxing the ξ value to 1.0 may work for intermediate and flexural links but would be less effective for shear links.

Fig. 4 illustrates how the introduction of the RLSs moves the location of plastic hinging

away from the link ends in W18x50 links. The figure plots the longitudinal plastic strain measured at the outer layer of the flange elements at mid-width of the flange, against the longitudinal location along the link. The strain values were measured at the stage when the links completed the first loading cycle that exceed their target plastic rotations (0.08 rad. for shear links, 0.05 rad. for intermediate links, and 0.02 rad. for flexural links). The figure shows that very large plastic strains are produced at the ends of unreduced links. By introducing RLSs with either $\xi = 0.86$ or 0.93, the location of severe plastic strains is shifted from the link end to within the RLS. For the intermediate and flexural links, the plastic strain at the link end is dramatically reduced by the introduction of RLSs. For the shear links, the plastic strain at the link ends remained fairly high but is significantly less than that for the unreduced case.

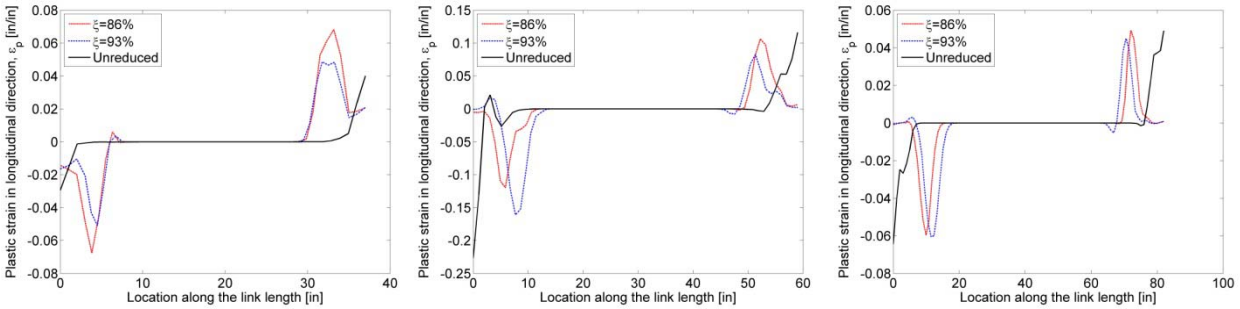

(a) (b) (c)

Figure 10. Plastic strain from the outer layer of the flange elements at mid-width of the flange vs. length along the link for the W18x50 links: (a) shear links, (b) intermediate links, (c) flexural links.

The effect of RLSs on shear links is further demonstrated in Fig. 11, which shows the deformed shape and plastic strain contours for the W18x50 shear links. Fig. 11a indicates that the large shear deformation imposes kinking deformation at the link ends, and thereby produces substantial secondary bending at the link flanges. Detailed finite element analyses by Okazaki (2004) showed that the secondary bending in the flanges of shear links can substantially increase the local plastic strains near the link ends. Figs. 11b and c clearly indicate that the introduction of the RLS moves the region of severe yielding and imposed kinking deformation away from the link end. Therefore, while not as clear as for intermediate and flexural links, the RLS may be quite effective for shear links.

Conclusions

To mitigate fracture at link-to-column connections in eccentrically braced frames, the concept of the reduced beam section has been applied, creating a reduced link section (RLS). A key design parameter of the RLS is the ratio of link end moment to the unreduced plastic moment capacity, denoted as ξ. Finite element analysis suggested that introduction of RLSs significantly reduces the plastic strain demands at the critical location for fracture, i.e., flanges at the link end, compared to the unreduced link. Reduction in plastic strain demand at that critical location should improve link ductility. The reduction was larger for intermediate and flexural links than it was for shear links. For shear links, larger reduction in flange plastic strain was obtained with lower values of ξ, while the strain reduction for intermediate and flexural links was not significantly affected by ξ.

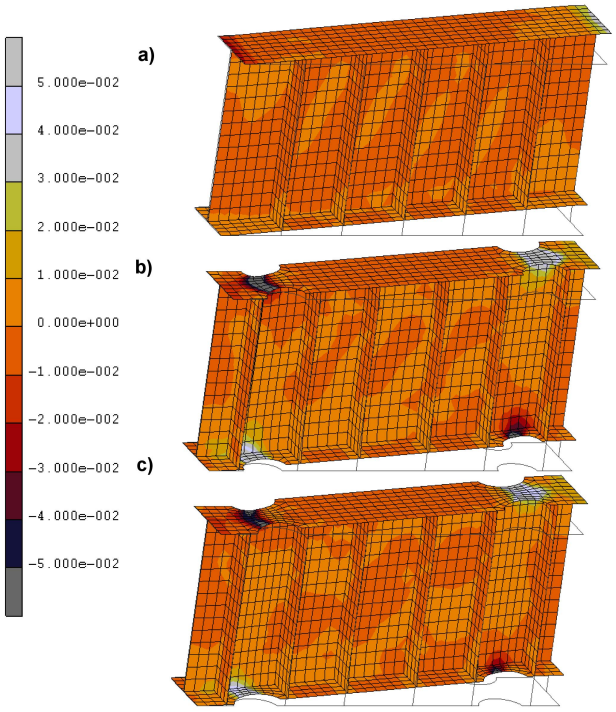

Figure 11. Plastic strain contours for the W18x50 shear links: (a) Unreduced section, (b) RLS section with $\xi = 0.86$, and (c) RLS section with $\xi = 0.93$.

References

AISC (2005a). *Seismic Provisions for Structural Steel Buildings, ANSI/AISC 341-05*, American Institute of Steel Construction, Chicago, IL.

AISC (2005b). *Prequalified Connections for Special and Intermediate Steel Moment Resisting Frames for Seismic Applications*, *ANSI/AISC 358-05*, American Institute of Steel Construction, Chicago, IL.

Berman, J.W., Hauksdottir, H.O., and Okazaki, T. (2010) "Reduced Link Sections for Improving the Ductility of Eccentrically Braced Frame Link-to-Column Connections" *Journal of Structural Engineering*, ASCE, (Accepted, In Press)

Choi, J., Stojadinovic, B., and Goel, S.C. (2003). "Design of free flange moment connection." *Engineering Journal*, AISC, 40(1), 25-41.

Hauksdottir, H.O. (2008). *Application of the Reduced Beam Section Concept for Improving the Ductility of Certain Eccentrically Braced Frames.* M.S. Thesis, University of Washington, Seattle, WA.

Kasai, K. and Popov, E.P. (1986). "General Behavior of WF Steel Shear Link Beams." *J. Struct. Div.* ASCE, 112(2): 362-382.

MSC Software (2005) *MSC. Marc User's Guide*, MSC.Software Corporation, Santa Ana, CA.

Okazaki, T. (2004). "Seismic performance of link-to-column connections in steel eccentrically braced frames." Ph.D. Dissertation, Department of Civil Engineering, University of Texas at Austin, Austin TX.

Okazaki, T., Engelhardt, M.D., Nakashima, M., and Suita, K. (2006). "Experimental Performance of Link-to-Column Connections in Eccentrically Braced Frames." *J. Struct. Eng.*, ASCE, 132(8): 1201-1211.